Fully renewable photocrosslinkable polycarbonates from cellulose-derived monomers

Sami Fadlallah, Aihemaiti Kayishaer, Mattia Annatelli, Louis Mouterde, Aurélien a M Peru, Fabio Aricò, Florent Allais

Fully renewable photocrosslinkable polycarbonates from cellulose-derived monomers

Sami Fadlallah,‡*[a] Aihemaiti Kayishaer,‡[a] Mattia Annatelli,‡[b] Louis M. M. Mouterde,[a] Aurélien A. M. Peru,[a] Fabio Aricò§*[b] and Florent Allais§*[a]

Cellulose-derived photocrosslinkable polycarbonates (PCs) with renewable citronellol pendant chains were synthesised through the polycondensation of Triol-citro, a recently developed levoglucosenone-based triol monomer, and dimethoxycarbonyl isosorbide. The polymer structures were unveiled through NMR spectroscopy and four repeating units were identified: three hydroxy-functional linear units (L_n, L_o and L_p) and one dendritic unit (D_q). The relative percentages of the repeating units, as well as the molecular weights of the corresponding polymers, can be finely tuned by varying the catalyst and reaction conditions (*i.e.,* polycondensation temperature and monomer concentration). Thermal analyses demonstrated that the novel PCs exhibited low glass transition temperatures (T_g as low as -72 °C) and $T_{d5\%}$ up to 159 °C. These hydroxy-functionalised PCs are not only fully biobased with a controlled extent of branching, but they also bear citronellol side chains that were successfully crosslinked *via* ultraviolet irradiation to further control the polymer properties.

Introduction

Applying the principles of Green Chemistry to polymer synthesis is extremely important to limit the extensive use of fossil-based resources (petroleum and natural gas), and to avoid large amounts of waste generated from the production processes.[1] Although renewability is not enough to identify a polymer/process as green,[2,3] the use of renewable raw materials (*e.g.,* biomass) not only meets the 4th principle of Green Chemistry[4] but also prompts the fabrication of low-carbon high-performing materials[5] from the discarded waste of biomass (140 Gt global annual generation).[6] For these reasons, the synthesis of green sustainable polymers has emerged as one of the hot topics of Biorefinery.[7]

Polycarbonates (PCs) are one of the most widely used engineering thermoplastics[8] that can be designed for a wide range of applications such as electrical instruments,[9] safety helmets, optical plates, and many others.[10–13] The global demand for PCs exceeds 4.4 million metric tons annually and is increasingly growing.[14] The most common production processes of PCs rely on the condensation polymerization of fossil-based chemicals, *i.e.*, bisphenol A (BPA) and phosgene. However, phosgene is extremely toxic by short-term inhalation exposure. Nowadays, the factories worldwide are strictly prohibited to produce and use phosgene. For these reasons, some industries (*e.g.*, Sabic Innovative Plastics, Bayer, etc.) have developed non-phosgene production processes of polycarbonates. This was also the scope of several research works in the past two decades.[15] Such approach is commonly based on the transesterification of dialkyl carbonates (*e.g.*, diphenyl carbonate (DPC)) with BPA. Nonetheless, BPA is a carcinogenic toxic molecule that has severe health effects[16] and should be replaced by sustainable and non-toxic alternatives.[17] A breakthrough development in new synthetic approaches to PCs was the copolymerisation of epoxides and CO_2 as a renewable carbonyl resource (Scheme 1A).[17]

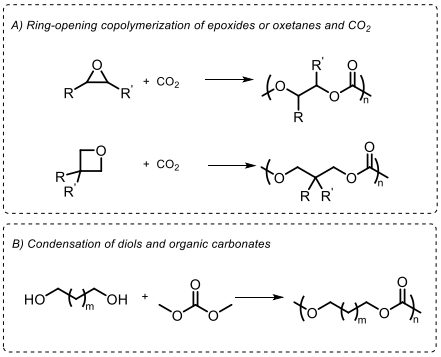

Scheme 1. Common potentially green production methods of polycarbonates

In this prospect, Coates *et al.* developed poly(limonene carbonate) from limonene oxide (a biobased epoxide) and CO_2 using a cobalt-based catalytic system.[18] Although this pioneering work[18] is of high interest, there is still plenty of room for improvement as cyclic monomers are rare and relatively expensive.

The condensation of hydroxy-containing monomers (diols, triols or polyols) and organic carbonates, *e.g.,* CO_2-derived dimethyl carbonate (DMC), is an attractive approach to produce PCs (Scheme 1B).[19] This method is endowed by the large availability of the bio-based hydroxy substrates as well as their easy preparation through green and cost-effective procedures. Among them,

isosorbide (Figure 1) is a rigid and non-toxic bicyclic C6 platform chemical[20–23] that has been employed in the synthesis of PCs,[24,25] as well as polyesters[26] and polyurethanes.[27] Isosorbide is not only glucose-derived compound that is commercially available but also cheap enough to be used in the production of biobased alternative PCs. Indeed, one of the biggest challenges in the biobased polymer market is making production cheap enough, but at the same time producing polymers with the desired properties to compete with fossil fuel counterparts. Notably, when compared to conventional PCs, isosorbide-based polycarbonates offer enhanced properties such as heat, scratch and UV resistance in addition to strength and other optical properties.[22,23,28]

Figure 1. Structure of isosorbide

The development of isosorbide-based PCs has been reported in several studies using DMC as an eco-friendly renewable carbonate source.[29–32] Nevertheless, the green synthesis of high molecular weight poly(isosorbide carbonate) is a challenge in industrial applications. Indeed, isosorbide possesses two hydroxy groups (*exo*-OH and *endo*-OH, Figure 1) with different reactivity, where the formation of intramolecular hydrogen bonds reduces the reactivity of the *endo*-OH.[33] Furthermore, the methylation of isosorbide by DMC can occur alongside the carboxymethylation and leads to termination, thus limiting the molecular weight of the polymers.[34] Recently, Zhang *et al.* proposed a metal-ion-mediated melt polycondensation method to modulate the reactivity of the two OH groups of isosorbide and to improve the selectivity of the carboxymethylation reaction.[34]

PCs were also prepared from dimethoxycarbonyl isosorbide (DCI) that can be achieved in high yield via methoxycarbonylation of isosorbide in the presence of dimethyl carbonate (DMC).[35] As an example, oligocarbonates vinyl esters and oligocarbonate polyols were prepared using DCI and its dimer.[36–39] The presence of functional groups, such as C=C, enhanced the performance of the polymers produced in the latter reports. Indeed, functional polymers offer the possibility to tune the thermal, mechanical and chemical properties of the corresponding polymers and enhance their performance towards a wider range of applications.[40] For instance, having additional free hydroxy groups in PC provides reactive sites for the attachment of bioactive molecules, flame retardants or crosslinking moieties. Gross *et al.* developed hydroxy-containing PCs through the enzyme-catalysed terpolymerisation of diethyl carbonate (DEC) with an aliphatic diol and a triol-based molecule that allowed polymer branching.[41] Very recently, we developed a green method to produce a highly valuable levoglucosenone(LGO)-derived triol monomer (Triol-citro) with citronellol side group (Scheme 2).[42] LGO is a cellulose-derived molecule[43,44] that received recently a great panel of attention as a platform to produce biobased polymers with different structures (*e.g.,* polyacetals,[45] polyacrylates,[46] polyolefins[47,48] and polyesters[49]) and glass transition (T_g) and thermal stability that cover a wide range of temperatures.[50] Furthermore, citronellol is a photocrosslinkable[51,52] naturally occurring monoterpenoid that is beneficial for wound healing applications such as tissue engineering.[53] LGO was used as a starting material to prepare a citronellol-containing five-membered lactone (HBO-citro) through a one-pot two-step pathway: i) acid-mediated oxa-Michael addition of citronellol to the highly reactive α,β-conjugated ketone of LGO, followed by ii) the in-situ solvent-free Baeyer-Villiger oxidation of LGO-citro (Scheme 2). Then, the full reduction of the lactone moiety led to the formation of Triol-citro in an 82% yield. Biodegradable and renewable branched polyesters with low T_g (-42 °C < T_g < -20 °C) were then prepared starting from this monomer (Scheme 2).[42]

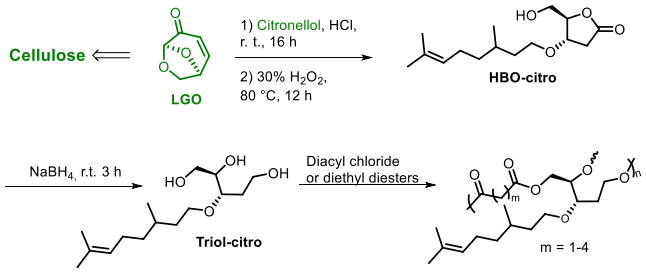

Scheme 2. Synthesis of fully renewable LGO-derived polyesters containing citronellol pendent group[42]

In the present study, through the polycondensation of bio-based Triol-citro and DCI, we extended the family of LGO-derived polymers to include, for the first time, functional PC structures having two reactive functional groups: citronellol and hydroxy. The effect of the catalyst nature, as well as that of the reaction conditions including temperature and the green LGO-derived solvent Cyrene™, on the PC structures were studied. Furthermore, the potential of the pendant citronellol moieties to undergo photocrosslinking upon ultraviolet (UV) irradiation was also examined. This work does not only give access to 100%

renewable PC architectures, but also introduces Triol-citro as a new versatile renewable platform to produce functional photocrosslinkable PCs using other carbonate resources.

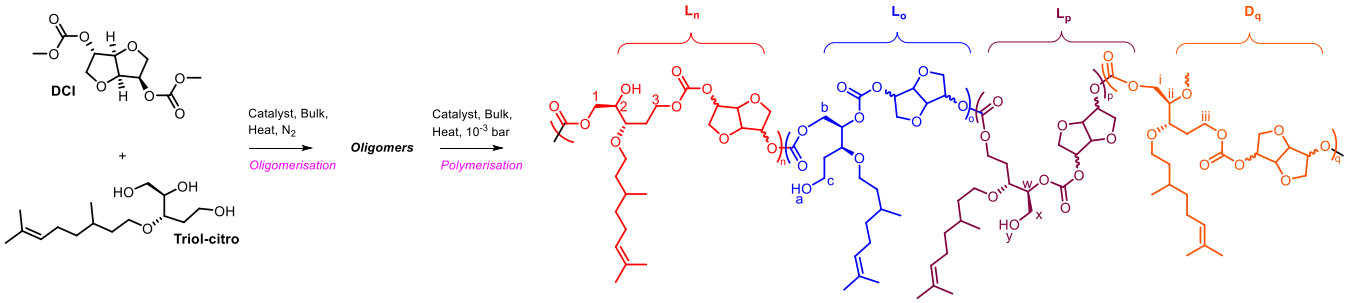

Scheme 3. Schematic representation of a PC structure synthesised through one-pot bulk polycondensation

Results and discussion

A series of solvent-free polycondensation reactions of Triol-citro and DCI (1.0 : 1.5 mol ratio), under different conditions (vide infra), was performed in three stages (Scheme 3). The first two stages were dedicated to the formation of oligomers (oligomerisation) under N2 and the third stage aimed at the condensation of the so-formed oligomers under vacuum (polymerisation). The oligomerisation stages are indispensable to form non-volatile short oligomers that can withstand reduced pressure, thus minimising monomer loss. The oligomerisation and polymerisation stages were conducted at different durations and temperatures to allow/maximize the formation of the PCs. The isolated polymers were found to be soluble in dimethylformamide (DMF) and dimethyl sulfoxide (DMSO).

Triol-citro is a chiral molecule that has three hydroxylic groups (two primary and one secondary) with different reactivities. Furthermore, DCI contains endo- and exo-carbonate groups that react differently. Thus, the polycondensation of Triol-citro and DCI leads to a very complex polymer structure. In the following section, we investigated by NMR and FTIR spectroscopy, the structures of the novel PCs. Indeed, such information is crucial to decipher the structure/property relationship of the polymer obtained under different conditions including type of catalyst (Table 1), temperature (Table 2) and monomer concentration (Table 3).

Structural characterization

Fourier-Transform Infra-Red (FTIR) analysis conducted on all the purified polymers showed two common features:

- an OH band at 3342 cm-1 that indicates the presence of unreacted hydroxylic moieties after the polycondensation;
- a vibration band of the carboxyl group at 1745 cm-1 attributed to the newly formed carbonate moieties along the polymer chains (e.g., Figures S10-S12, Supporting Information (SI)).

Furthermore, an accurate evaluation of the PCs NMR spectra allowed the identification of four repeating units: three linear units (Ln, Lo and Lp) incorporating pendant hydroxy groups and one branched unit (Dq) resulting from the reaction of the three hydroxy groups of Triol-citro with the DCI carbonates moieties (Scheme 3 and Figure 2). The signals at {4.43 (H1-syn), 4.35 (H2) and 4.13 ppm (H1-anti)}, {4.72 (Ha), 4.48 (Hb-syn), 4.23 (Hb-anti) and 3.81 ppm (Hc)}, {4.73 (Hw), 3.94 (Hy), 3.69 (Hx-syn) and 3.64 ppm (Hx-anti)} and {4.48 (Hi-syn), 4.33 (Hii) and 4.23 (Hi-anti)} can be attributed to Ln, Lo, Lp and Dq, respectively (Figure 2).

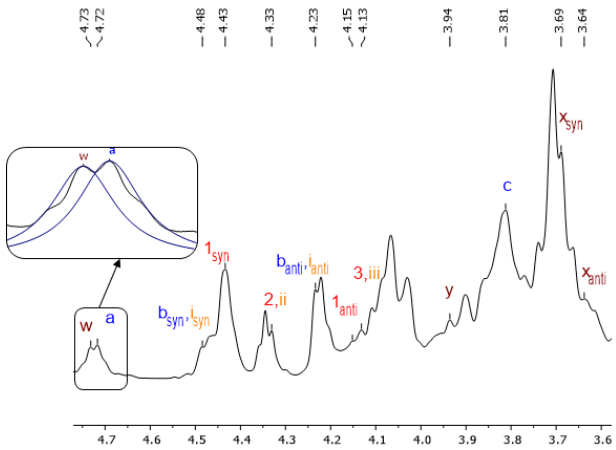

Figure 2. Typical ^{1}H NMR (DMSO-d_6) spectrum of the PC structure (#7, Table 1) shown in Scheme 3 (see SI for the full ^{1}H-NMR spectrum)

The correlation between the different signals was confirmed by 2D NMR spectroscopy, especially ^{1}H-^{13}C HSQC. The intact olefin bond of the citronellol side chains is visible at 5.06 ppm (^{1}H NMR, Figure S7, SI), 130.9 and 125.0 ppm (^{13}C NMR, Figure S8, SI).

As expected, the carbonate groups of the PC structure gave multiple peaks (more than 12 signals) in ^{13}C NMR in the 155.2-153.5 ppm region due to the overall six stereogenic centers present in the starting monomers (Triol-citro and DCI) as well as to the remarkable different reactivity of the functional groups taking part to the polycondensation.

In our previous work when the polymerisation of DCI was conducted by reaction with an excess of DMC (10 eq.), the ^{13}C spectrum displayed only three C=O signals with intensity ratios of 1:2:1 corresponding to the *endo-endo*, *endo-exo/exo-endo*, and *exo-exo* carbonate groups, respectively.[54]

Table 1. Polycondensation of Triol-citro and DCI: catalysts screening

Run#	Catalyst[a]	Yield (%)[b]	M_n (kDa)[c]	$Đ$[c]	T_g (°C)[d]	$T_{d5\%}$ (°C)[e]	L_n unit (%)[f]	L_o unit (%)[f]	L_p unit (%)[f]	∑L (%)[f]	D_q unit (%)[f]
1	-	63	2.3	1.58	*mv*[g]	129	92	2	5	99	1
2	LiAcac	68	2.5	1.17	-69	126	57	3	14	74	26
3	Li_2CO_3	76	2.9	2.10	-60	144	63	18	13	94	6
4	Na_2CO_3	70	2.4	1.46	-72	127	11	81	2	94	6
5	K_2CO_3	65	2.8	1.67	-72	132	13	80	5	98	2
6	Cs_2CO_3	88	23.4	2.05	-60	154	25	21	7	53	47
7	$Ti(OBu)_4$	66	7.9	1.49	-40	136	41	3	40	84	16
8	$Zn(OAc)_2$	73	21.4	1.64	-54	118	37	7	31	75	25

[a] Triol-citro : DCI in 1.0 : 1.5 mol ratio; 2 mol% of catalyst; Temperature of polymerization stage (3rd stage) = 220 °C. [b] Isolated yield of the product, % yield = (isolated mass/theoretical mass) *x* 100. [c] Determined in DMF (10 mM LiBr) at 50 °C. [d] Glass transition temperature determined by DSC. [e] TGA degradation temperature at which 5% ($T_{d5\%}$) mass loss was observed under nitrogen. [f] Measured quantitatively by the deconvolution of the ^{1}H NMR spectra. [g] mv = multiple values; Three T_g values were observed by DSC: -41, -28 and -14 °C.

In an attempt to quantitatively determine the relative fractions (in %) of the repetitive units of the PC structures, the deconvolution of the ^{1}H NMR spectra was performed to separate the overlapping peaks and determine the corresponding area and intensity of each signal.

The relative percentages of the linear and dendritic units were obtained according to the following equations (1-4), where the subscript "A" indicates the area of the deconvoluted proton NMR signal within the brackets.

$$(1) \qquad \%\, L_n\ units = \frac{[2]_A \times 100}{[2]_A + [a]_A + [w]_A + [iii]_A}$$

$$(2) \qquad \%\, L_o\ units = \frac{[a]_A \times 100}{[2]_A + [a]_A + [w]_A + [iii]_A}$$

$$(3) \qquad \%\, L_p\ units = \frac{[w]_A \times 100}{[2]_A + [a]_A + [w]_A + [iii]_A}$$

$$(4) \qquad \%\, D_q\ units = \frac{[iii]_A \times 100}{[2]_A + [a]_A + [w]_A + [iii]_A}$$

It should be noted that, for a better evaluation of the aforementioned percentages, the terminal units should also be considered. However, the very complex structure of the polymers, as well as the high number of possible terminal units, precluded a definite assignment of the related chemical shifts. The Degree of branching (DB) indicates the percentage of dendritic units based on the total number of repeating units. DB is calculated according to equation (5) where ∑D and ∑L represent the summation of the dendritic and linear units, respectively. More precisely, $\sum D = D_q$ and $\sum L = L_n + L_o + L_p$. As the calculation of the percentage of terminal units was out of reach in this study, DB is then assumed to be equal to the percentage of D_q units along the polymer chain.

$$DB = \frac{\sum D \times 100}{\sum L + \sum D} \quad (5)$$

According to the above-discussed calculation, Tables 1-3 report the microstructural determination of all the prepared PCs. The details will be discussed in the following sections based on the polymerisation reaction conditions.

Catalyst screening

Several metal-based catalysts, *i.e.,* LiAcac, Li_2CO_3, Na_2CO_3, K_2CO_3, Cs_2CO_3, $Ti(OBu)_4$ and $Zn(OAc)_2$, were used to promote the synthesis of PCs. The alkali carbonate catalysts were chosen based on a study by Shin *et al.* who showed that the nature of the alkali metal affects the preparation and properties of the isosorbide-derived PCs.[55] Furthermore, an alkali metal acetylacetonates such as LiAcac was selected according to the results reported by Zheng *et al.* which showed an exceptional activity of LiAcac towards the preparation of isosorbide-based homo- and Co-PCs especially when compared to $Ti(OBu)_4$ and $Zn(OAc)_2$.[29]

All polycondensation experiments of Table 1 were conducted in successive three steps to allow the formation of polymers: i) under N_2 atmosphere at 100 °C for 18 h, then ii) the temperature was gradually increased to 160°C and left to stir for 3 h, followed by iii) a further increase in temperature to reach 220 °C where a high vacuum (10^{-3} bar) was applied for 2 h.

Table 1 summarizes the molecular weight (M_n), dispersity ($Đ$) and thermal properties (*i.e.*, glass transition (T_g) and 5% mass loss temperature ($T_{d5\%}$)) of the PCs obtained when Triol-citro and DCI were reacted in the presence of 2 mol% of the selected catalysts. The percentage of the relative fractions of the constituting units (L_n, L_o, L_p and D_q) was also evaluated.

Noticeably, the presence and nature of the catalyst had a significant influence on the polymer composition. A poignant example is the catalyst-free polymerisation that led to a PC incorporating mostly linear units. More precisely, the polymer is composed of 92% of L_n units as a result of the condensation reaction between the two more reactive primary hydroxy groups of Triol-citro with the DCI methylcarbonate units. If all linear units are considered, ∑L was 99%; thus, under these conditions only 1% of branched structures (D_q) were detected.

On the other hand, when LiAcac was employed as catalyst (2 mol%) D_q reached a value of 26%. This observation demonstrates the importance of a basic catalyst to activate the less-nucleophilic secondary hydroxy group of Triol-citro towards the (poly)condensation reaction. Furthermore, the nature of the catalyst can be highlighted by examining the results of experiments 2-8 reported in Table 1. Dendritic structures with D_q = 16%, 25%, 26% and 47% were obtained with $Ti(OBu)_4$, $Zn(OAc)_2$, LiAcac and Cs_2CO_3, respectively. However, in the presence of weaker bases such as K_2CO_3, Li_2CO_3 and Na_2CO_3, the dendritic ratio (D_q) in the polymer backbone was minimal, 2%, 6% and 6%, respectively. The latter were accompanied by an increase of the linear units to reach ∑L = 98%, 95% and 94%, respectively. Furthermore, it was found that the nature of the metal catalyst can remarkably influence the reactivity of the present hydroxy groups of Triol-citro *(vide infra)* which in turn affect the proportions of the three linear units (L_n, L_o and L_p, Scheme 3). For instance, if L_o unit is taken as an example, the following catalysts Li_2CO_3 and Na_2CO_3 led to the formation PCs structures with an increased percentage of L_o, *ca.* 18% up to 81% (see Table 1 for more details).

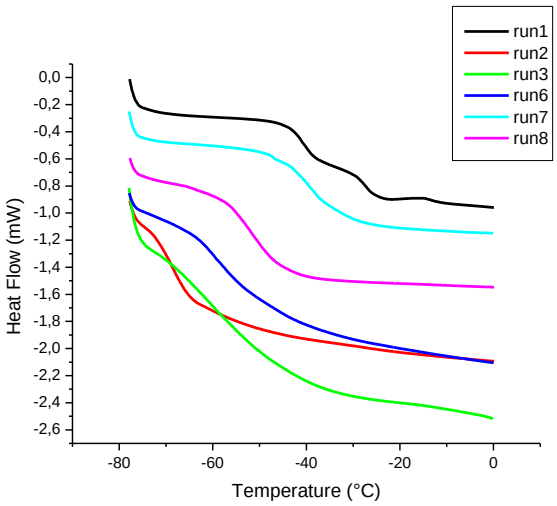

Figure 3. DSC thermograms of the PCs herein prepared; the run numbers correspond to the experiments 1-8 reported in Table 1

A short polymer with M_n = 2.5 kDa was obtained using LiAcac (#2, Table 1); this result differs from the high molecular weight isosorbide-based PCs that was previously achieved using this catalyst.[29] Indeed, the catalyst-free oligomerization reaction gave a similar M_n value (2.3 kDa) (#1, Table 1). Nonetheless, differential scanning calorimetry (DSC) analysis showed, for the latter polymerisation, three T_g VALUES AT -41, -28 and -14 °C due to the uncontrolled transesterification reactions in the absence of a catalyst (Figure 3). On the other hand, all the other PCs (#2-8; Table 1) showed single negative T_g values in the range of -72 °C to -40 °C (Figure 3). Indeed, the presence of citronellol side groups led to low T_g that are useful for biomedical applications that necessitate polymers with T_g lower than body temperature. Similar behavior was observed for the citronellol-bearing polyesters (-42 °C < T_g < -20 °C)[42] as well as for the polyphosphazenes-citronellol polymers that showed a T_g as low as -88 °C.[51,52]

Interestingly, polymers with M_n up to 23.4 and 21.4 kDa were detected in the case of Cs_2CO_3- and $Zn(OAc)_2$-catalysed polycondensations, respectively (#6 and #8; Table 1). This remarkable reactivity of Cs_2CO_3 was already observed by Shin *et al.* in the melt polymerisation of isosorbide-based polycarbonates.[55] They showed that among the different alkali carbonate catalysts, Cs_2CO_3 showed the highest catalytic activity and only a small amount (*i.e.,* 0.2 ppm) was sufficient to produce polycarbonate with M_n = 26.7 kDa.[55] Most probably this could be ascribed to i) the higher basicity of cesium carbonates when compared with analogous alkali carbonates, ii) the larger cationic radius and electronic polarizability of Cs^+ ion, and iii) the lowest degree of solvation and ion-pairing of Cs^+.[55] In this view, it can be hypothesised that in the polycondensation of Triol-citro and DCI, the first step involves the dissociation of Cs_2CO_3 to a free Cs^+ ion able to coordinate the carbonate sp^2 oxygen of a DCI molecule. Due to the high polarizability of the Cs^+ ion, the carbonyl groups of DCI become more electrophilic and thus more easily attacked by the primary and secondary hydroxyl groups of Triol-citro (Scheme 4).

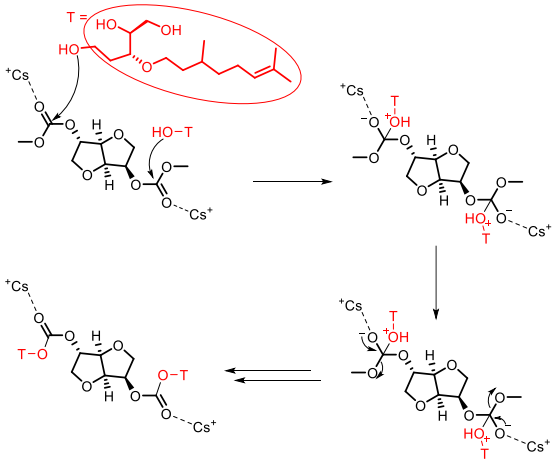

Scheme 4. Polycondensation mechanism of Triol-Citro and DCI catalysed by Cs_2CO_3

Thermogravimetric analyses (TGA) showed that the LiAcac-catalysed reaction led to a polymer with $T_{d5\%}$ of 126 °C (#2; Table 1), whereas the $T_{d5\%}$ of the PC obtained without catalyst (#1, Table 1) was 129 °C. However, higher $T_{d5\%}$ of 144 and 154 °C were obtained with Li_2CO_3 and Cs_2CO_3.

Table 2. Polycondensation of Triol-citro and DCI: effect of temperature of the polymerisation stage

Run#	T (°C)[a]	Yield (%)[b]	M_n (kDa)[c]	$Đ$[c]	T_g (°C)[d]	$T_{d5\%}$ (°C)[e]	L_n unit (%)[f]	L_o unit (%)[f]	L_p unit (%)[f]	∑L (%)[f]	D_q unit (%)[f]
9	160	85	1.4	1.20	-40	159	43	7	21	71	29
10	180	78	1.3	1.08	-51	138	39	30	9	78	22
11	200	75	2.9	1.29	-62	132	1	40	27	68	32
12	240	70	27.3	1.20	-70	115	53	23	18	94	6
13	250	72	2.5	1.81	-72	99	27	25	39	91	9

[a] Temperature of the polymerisation stage (3rd stage), See #6, Table 1 for the experiment performed at 220 °C. [b] Isolated yield of the product, % yield = (isolated mass/theoretical mass) *x* 100. [c] Determined in DMF (10 mM LiBr) at 50 °C. [d] Glass transition temperature determined by DSC. [e] TGA degradation temperature at which 5% ($T_{d5\%}$) mass loss was observed under nitrogen. [f] Measured quantitatively by the deconvolution of the ^{1}H NMR spectra.

Table 3. Polycondensation of Triol-citro and DCI in Cyrene™: solvent effect

Run#	[Monomers] (M)[a]	Yield (%)[b]	M_n (kDa)[c]	$Đ$[c]	T_g (°C)[d]	$T_{d5\%}$ (°C)[e]	L_n unit (%)[f]	L_o unit (%)[f]	L_p unit (%)[f]	D_q unit (%)[f]
14	2	56	682.2	1.05	-	131	59	10	17	14
15	4	34	20.7	1.91	-	148	65	7	11	17
16	8	31	19.2	1.41	-	147	63	5	3	29

[a] Concentration of Triol-citro and DCI. [b] Isolated yield of the product, % yield = (isolated mass/theoretical mass) *x* 100. [c] Determined in DMF (10 mM LiBr) at 50 °C. [d] No glass transition temperature was determined by DSC. [e] TGA degradation temperature at which 5% ($T_{d5\%}$) mass loss was observed under nitrogen. [f] Measured quantitatively by the deconvolution of the ^{1}H NMR spectra.

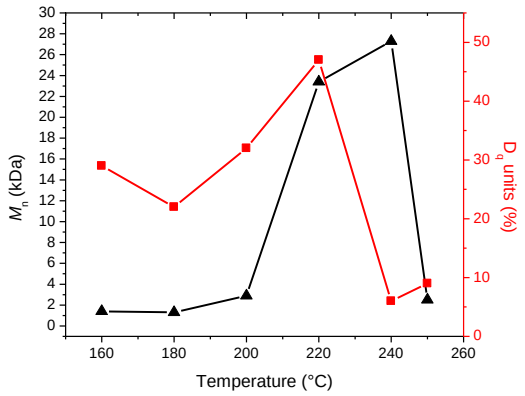

Figure 4. Effect of polycondensation temperature on M_n and polymer branching

Effect of temperature

According to the data reported in Table 1, Cs2CO3 was selected as the best catalyst for further studies. In particular, the effect of the temperature on the polymerisation stage - previously conducted at 220 °C (#6; Table 1) - was next investigated. It has been previously reported that a temperature higher than 190 °C is required to activate the metal-based catalyst in this type of polycondensation reactions.29 However, in order to have a better insight on the effect of the temperature on the PC properties a series of experiments were conducted at 160, 180, 200, 240 and 250 °C (Table 2).

Figure 4 shows the influence of the polycondensation temperature on the Mn values. The Mn grew slightly from 1.4 to 2.9 kDa with the temperature increasing from 160 to 200 °C. A significant rise from 2.9 to 27.3 kDa was then observed when the reaction was conducted at 200 and 240 °C, respectively. The PCs Mn decreased in the 240-250 °C range to reach 2.5 kDa.

In conclusion, the optimum M_n value for the Cs_2CO_3-catalysed polycondensation of Triol-citro and DCI was achieved at 240 °C. Similar behavior was reported by Zheng *et al.* who used LiAcac as a catalyst.[29] On the other hand, if the polymer composition is taken as a criterion (Figure 4), an increase of the total average linear units (∑L) from 68% to 94% was observed at temperatures ranging from 200 to 240 °C.

Therefore, taking in consideration both M_n and polymer composition, data collected suggest that 220 °C is the best choice for the formation of long polymers with a more hyperbranched structure, whereas, long linear PCs and short hyperbranched ones can be obtained at 200 and 240 °C, respectively. It should be also mentioned that the tested conditions (catalyst screening and temperature) not only allow tuning the linearity *vs.* branching of the polymers, but also lead to OH-functionalised polymers with three hydroxyl groups that have different reactivities depending on the L units.

Effect of monomer concentration

The hydrogenation of the conjugated double bond of LGO produces Cyrene™ which is used as a green aprotic polar solvent for various synthetic reactions.[56] The potential of Cyrene™ as a bio-based solvent for polymer syntheses has been recently explored.[47,57–59] Among the few reported studies, Pellis et *al*. showed that Cyrene™ can be used as a medium for the preparation of sustainable galactarate-based polyesters through an enzyme-catalysed process.[58] Also, recently, the same research group showed the applications of Cyrene™ and its derivative Cygnet 0.0 as a safer replacement for polar aprotic solvents in polymerization reactions.[60]

To the best of our knowledge, no study has been yet reported on the use of Cyrene™ for the synthesis of polycarbonates. In this view, we decided to explore this media in the Cs_2CO_3-mediated polycondensation of Triol-citro and DCI especially in consideration of the fact that Cs_2CO_3 has superior solubility in polar aprotic solvents.[55]

The polymerisation procedure was slightly adapted to avoid the evaporation of Cyrene™, whose boiling point is 227 °C under atmospheric pressure. The polymerisations were then performed according to the following three stages:

- stage 1 - 100 °C under 0.5 bar for 18 h;
- stage 2 - 180 °C under 0.2 bar for 2 h;

- stage 3 - 200 °C under 0.006 bar for 4 h.

Three monomer concentrations were tested, *i.e.*, 2, 4 and 8 M based on both Triol-citro and DCI (Table 3). Interestingly, for 2 M solution polymerisation, the SEC analysis showed a peak at 9.86 min that belongs to a polymer having an M_n of 682.2 kDa (Figure S18, SI). The M_n difference of PCs synthesised in solution *vs.* in bulk might be ascribed to i) the better homogenization of the reaction mixture at the early stage of the polymerisation, and ii) the enhanced solubility, thanks to the presence of Cyrene™, of Cs_2CO_3 as well as the oligomers/polymers produced. Indeed, increasing the monomer concentration to 4 and 8 M gave similar results to bulk polymerisation in terms of M_n (20.7 and 19.2 vs. 23.4 kDa). Noticeably, the presence of Cyrene™ enhanced the formation of linear units having secondary hydroxy groups (L_n) along the polymer chain. The percentage of L_n units of the 2, 4 and 8 M solutions were 59%, 65% and 63%, respectively. These values are more than twice the L_n obtained for solvent-free polymerisation (25%).

Concerning T_g, no heat flow variations were recorded in the range of -80 °C to 160 °C. Nevertheless, TGA analysis showed similar thermal stability as in the case of bulk polymerisation (Table 3).

UV crosslinking of the citronellol side chains

To evaluate the effect of crosslinking of the citronellol pendant chains on the properties of the PCs, a polymer sample (PC-6, #6, Table 1) was irradiated with UV light (400 W, 300 nm) (Scheme 5). The efficiency of the UV crosslinking was firstly monitored by proton NMR.

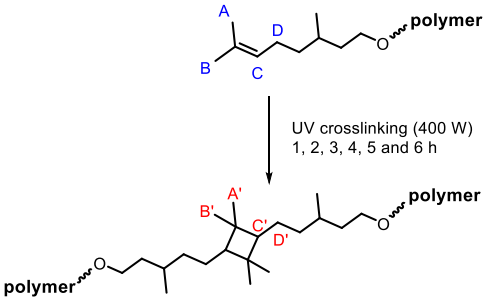

Scheme 5. Representation of the UV-crosslinked citronellol moiety

Figure 5 shows the impact of the increased time to UV exposure on the crosslinking evolution of PC-6 evaluated via 1H-NMR. The first prominent observation is the progressive disappearance of the C=CH peak (HC) of citronellol at 5.07 ppm as the irradiation time increased. This was accompanied by the gradual appearance of HC' at 2.07 ppm due to the formation of the C-C bond. The latter also resulted in an upfield shift of the protons HD and HA from 1.92 and 1.56 ppm to 1.63 and 1.19 ppm, respectively.

Furthermore, 13C NMR analysis of PC-6 after 6 h irradiation confirmed the complete disappearance of the C=C peaks at 131 and 125 ppm. To calculate the percentage of crosslinking of PC-6, the integration of the olefin peak at 5.07 ppm (Hc) was taken as a reference based on the CH3 signal at 0.82 ppm.

The % of crosslinking was determined according to the following equation, where t represents the duration of UV irradiation and the brackets the integral of proton HC' at a predetermined time.

$$Percentage\ of\ crosslinking = 100 - \frac{[H_{C'}]_t \times 100}{[H_{C'}]_o}$$

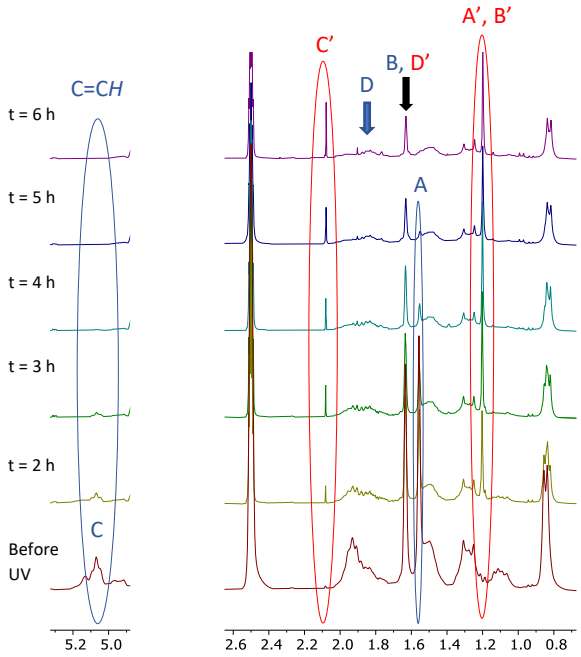

Figure 5. Monitoring of ^{1}H NMR (DMSO-d_6) spectra of a PC sample (# 6, Table 1) after 2-6 h of exposure to UV irradiation (400 W)

Figure 6 reports the increase of the crosslinking extent with increasing UV time exposure. These results confirm the successful crosslinking of the citronellol moieties of PC-6 to yield a highly crosslinked hyperbranched structure.

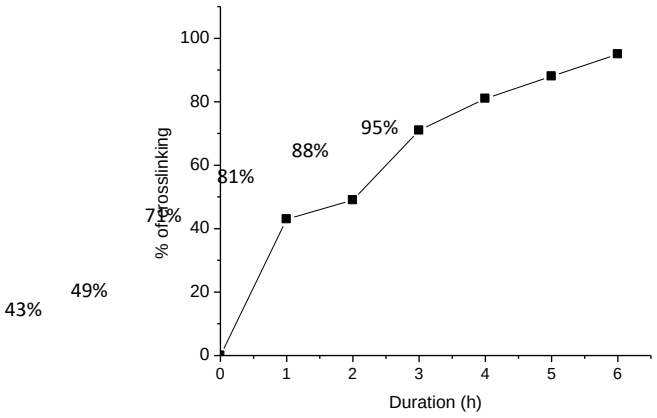

Figure 6. Evolution of % of crosslinking of PC-6 vs the duration of UV irradiation

The molecular weight of the photocrosslinked material was then analysed by SEC analysis. The limited solubility of the polymer in DMF after crosslinking prohibited us from following the change in Mn values. Nevertheless, SEC analysis of the soluble portions displayed Mn in the 0.8-0.9 kDa range (Figures S21 and S22, SI).

DSC analysis showed a noticeable increase of Tg from -60 °C to -6 °C after irradiating PC-6 by UV for 6 h (Figures S28 and S36, SI). Indeed, as the degree of crosslinking within a given polymer structure increases, the mobility of the network chains decreases, resulting in a less flexible/more rigid structure with a higher Tg value.

The TGA analysis was also performed to check whether the photo-induced crosslinking increased the thermal stability. Td5% was enhanced to reach 163 °C due to the formation of a more rigid structure - Td5% of the uncrosslinked structure was 154 °C. The higher thermal stability was even more representative if Td50% is

considered (the temperature at which 50% mass loss occurred) where a considerable increase from 212 °C to 444 °C was recorded after UV irradiation (Figure S50, SI).

Conclusions

LGO was recently used as a renewable substrate to produce Triol-citro. The solvent-free polycondensation of Triol-citro with dimethoxycarbonyl isosorbide (DCI) led to novel PCs incorporating linear (Ln, Lo and Lp) and dendritic (Dq) units. Within the PC backbone, the percentages of linear (Ln, Lo and Lp) vs. dendritic (Dq) were dependent on the chosen catalyst and polymerisation conditions. The Cs2CO3-catalysed polycondensation afforded a hyperbranched structure. On the other hand, when catalyst-free or K2CO3-mediated polymerisations were investigated, linear oligomers were obtained. Screening of polycondensation temperature showed that the optimum outcome depends on the chosen criteria (Mn or/and polymer composition). Solution polymerisations were investigated in Cyrene™ as a green cellulose-derived solvent. Although the polymers were isolated in low yields, high molecular weight polymers with Mn = 682.2 kDa were detected for the 2 M solution polymerisation.
Furthermore, the UV-induced crosslinking of the citronellol side chains of PC-6 was investigated. The polymer crosslinking was monitored by NMR and showed that exposure to UV irradiation for 6 h was enough to crosslink 95% of the citronellol moieties, resulting in an increase of Tg from -60 °C to -6 °C and of Td50% from 212 °C to 444 °C.
Although the PCs reported in this study possess lower Tg values than the BPA-based PCs. These polymers can be used in biomedical applications that require low Tg materials. Furthermore, the new approach paves the way for the development of new family of LGO-derived triols that can be prepared by the straightforward oxa-Michael addition of alcohols having different chains. The length of the side chains can thus affect/control the Tg of the corresponding polycarbonates. These prospects are currently under investigation, as well as the use of other renewable organic biscarbonates rather than DCI.

Experimental section

Chemical and reagents. Levoglucosenone and Cyrene™ were graciously provided by Circa group. Citronellol (Sigma-Aldrich), sodium borohydride >98% (Sigma-Aldrich), zinc(II) acetate >99% (Acros Organic), titanium(IV) butoxide 99+% (Fisher), cesium carbonate 99.5% (Fisher), lithium carbonate 99.99% (Fisher), potassium carbonate 99% (Sigma-Aldrich), sodium carbonate (VWR), (2,4-pentanedionato)lithium (TCI). HPLC grade solvents were purchased from Thermofisher Scientific and used as received. NMR solvents including $CDCl_3$ and DMSO-d_6 were purchased from Cambridge Isotopes Laboratories. Ultra-pure laboratory-grade water was obtained from MilliQ, 18.2 megaOhms. TLC analyses were performed on an aluminum strip coated with Silica Gel 60 F254 from Merck, revealed under UV-light (254 nm) then in presence of potassium permanganate staining solution. All manipulations with air-sensitive chemicals and reagents were performed using standard Schlenk techniques on a dual-manifold line, on a high-vacuum line.

Characterization

Nuclear Magnetic Resonance (NMR) spectroscopy. ^{1}H NMR spectra were recorded on a Bruker Fourier 300 MHz ($CDCl_3$ residual signal at 7.26 ppm and DMSO-d_6 residual signal at 2.5 ppm). ^{13}C NMR spectra were recorded on a Bruker Fourier 300 (75 MHz) ($CDCl_3$ residual signal at 77.16 ppm and DMSO-d_6 residual signal at 39.52 ppm). Data are reported as follows: chemical shift (δ ppm), assignment. All NMR assignments were also made using ^{1}H-^{1}H COSY, ^{1}H-^{13}C HMBC and ^{1}H-^{13}C HSQC spectra.

Size exclusion chromatography (SEC) was performed at 50 °C using an Agilent Technologies 1260 Infinity Series liquid chromatography system with an internal differential refractive index detector, a viscometer detector, a laser and two PLgel columns (5 µm MIXED-D 300 x 7.5 mm) using 10 mM Lithium Bromide in HPLC grade dimethylformamide as the mobile phase at a flow rate of 1.0 mL/min. Calibration was performed with poly(methyl methacrylate) standards from Agilent Technologies.

Thermogravimetric Analysis (TGA) was measured with a TGA Q500 (TA Instruments). Typically, ~2 mg of each sample was equilibrated at 50 °C for 30 min and was flushed with highly pure nitrogen gas. All the experiments were performed with a heating rate of 10 °C/min up to 500 °C. The reported values of $T_{d5\%}$ and $T_{d50\%}$ represent the temperature at which 5% and 50% of the mass is lost respectively. Concerning the normalization of TGA, a slight shift in some cases took place during the isothermal step at 50 °C which is necessary to stabilize the sample in the

oven prior to analysis. The corresponding degradation temperatures reported in this manuscript consider this slight shift while calculating $T_{d5\%}$ and $T_{d50\%}$ of the reported polymers.

Differential Scanning Calorimetry (DSC) was performed with a DSC Q20 (TA Instruments). Typically, ~8 mg sample was placed in a sealed pan, flushed with highly pure nitrogen gas and passed through a heat-cool-heat cycle at 10 °C/min in a temperature range of -80 °C to 120 °C. Three heat/cool cycles were done for each sample where the last two cycles were dedicated to analyzing the heat flow of the sample after being cooled in controlled conditions. The T_g values recorded herein are those obtained from the third cycle.

Fourier-transform infrared spectroscopy (FTIR) was recorded on a Cary 630 FTIR Spectrometer by Agilent (Wilmington, DE, USA).

Synthesis of HBO-citro. A biphasic mixture of LGO (50 g, 0.4 mol), citronellol (512 mL, 1.8 mol) and HCl (5 N, 0.6 mol) was stirred at room temperature for 16 h. The resulting mixture was cooled down with an ice bath followed by dropwise addition of a 30% solution of H_2O_2 (2 mL) for 2 h. After completion of the addition, the reaction was heated up to 80 °C and stirred for 12 h. The presence of H_2O_2 was evaluated with peroxide strips and, if any, the residual H_2O_2 was quenched using sodium sulfite. The reaction was extracted with ethyl acetate (two times). Organic layers were washed with brine, dried over anhydrous $MgSO_4$, filtered and evaporated to dryness. This step was followed by distillation to remove excess citronellol. The crude product was purified by flash chromatography (gradient 90/10 to 20/80, cyclohexane/ethyl acetate as eluant) to give 62 g of HBO-citro as a pale-yellow oil (58%).

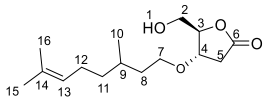

^{1}H NMR (δ ppm, $CDCl_3$): 5.01 (broad t, J = 5.19 Hz, 1H, H_{13}), 4.43 (s, 1H, H_3), 4.11 (d, J = 7.0 Hz, 1H, OH), 3.84 (dd, J = 3.3 and 12.4 Hz, 1H, H_4), 3.65 (dd, J = 3.3 and 12.4 Hz, 2H, H_2), 3.39 (m, 2H, H_7), 2.81 (dd, J = 7.0 and 18.1 Hz, 1H, H_{5a}), 2.44 (dd, J = 3.3 and 18.1 Hz, 1H, H_{5s}), 1.90 (m, 2H, H_{12}), 1.61 (s, 3H, H_{15}), 1.53 (s, 3H, H_{16}), 1.27-1.07 (m, 4H, H_{11}, H_8), 0.82 (d, J = 6.4 Hz, 3H, H_{10}).

^{13}C NMR (δ ppm, $CDCl_3$): 176.7 (C_6), 131.2 (C_{14}), 124.6 (C_{13}), 85.9 (C_3), 76.1 (C_4), 67.6 (C_7), 62.1 (C_2), 37.1 (C_{11}), 36.5 (C_8), 35.9 (C_5), 29.3 (C_9), 25.7 (C_{15}), 25.3 (C_{12}), 19.4 (C_{10}) 17.6 (C_{16}).

Synthesis of monomers

Triol-citro. An aqueous solution of sodium borohydride (1.14 g in 3 mL of water, 30 mmol) was added dropwise to a solution of HBO-citro (4.5 g, 15 mmol) in THF (60 mL) in a water-ice bath. The reaction mixture was stirred at room temperature for 3 h. The reaction was quenched with acetone and a 20% aqueous solution of citric acid (20 mL). The reaction was extracted twice with ethyl acetate. Organic layers were washed with brine, dried over anhydrous magnesium sulfate, filtered and evaporated to dryness. The crude product was purified by flash chromatography (gradient 90/10 to 20/80, cyclohexane/ethyl acetate as eluant) to give 3.39 g of Triol-citro as a colorless oil (82%).

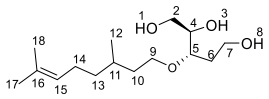

^{1}H NMR (δ ppm, DMSO-d_6): 5.07 (t, J = 7.2 Hz, 1H, H_{15}), 4.55 (s, OH), 4.38 (s, OH), 4.34 (s, OH), 3.50-3.27 (broad, m, 8H, H_9, H_7, H_5, H_4, H_2), 1.93 (broad, m, 2H, H_{14}), 1.64 (s, 3H, H_{17}), 1.56 (s, 3H, H_{18}), 1.50-1.10 (broad, m, 5H, H_{13}, H_{11}, H_{10}), 0.84 (d, J = 6.2 Hz, 3H, H_{12}).

^{13}C NMR (δ ppm, DMSO-d_6): 130.8 (C_{16}), 125.1 (C_{15}), 77.7 (C_5), 73.5 (C_4), 67.9 (C_9), 63.4 (C_2), 58.2 (C_7), 37.3 (C_{13}), 37.1 (C_{10}), 33.9 (C_6), 29.2 (C_{11}), 25.9 (C_{17}), 25.4 (C_{14}), 19.8 (C_{12}), 17.9 (C_{18}).

DCI. In a 250 mL double-necked bottom round flask equipped with a Dena-Stark trap and condenser, 5 g of isosorbide (34.21 mmol) was reacted with 90 mL of dimethyl carbonate (1.07 mol) in presence of 0.95 g of K_2CO_3 as a base (6.80 mmol), at 90 °C for 6 h. After cooling, the reaction crude was filtered and concentrated in vacuo to

provide DCI in quantitative yield. A pure sample of DCI was obtained *via* column chromatography using DCM/MeOH (99/4).

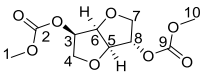

^{1}H NMR (δ ppm, DMSO-d_6): 5.03 (q, J = 4.8 Hz, 1H, H_3), 4.96 (d, J = 3.2 Hz, 1H, H_8), 4.81 (t, J = 5.4 Hz, 1H, H_6), 4.45 (d, J = 5.0 Hz, 1H, H_5), 3.95 (d, J = 10.9 Hz, 1H, H_7), 3.81 (d, J = 4.2 Hz, 2H, H_4), 3.77 (d, J = 3.3 Hz, 1H, H_7), 3.72 (d, J = 1.6 Hz, 6H, H_1, H_{10}).

^{13}C NMR (δ ppm, DMSO-d_6): 155.0 (C_2), 154.7 (C_9), 85.7 (C_5), 82.1 (C_6), 81.1 (C_8), 81.0 (C_3), 77.1 (C_7), 70.7 (C_4), 55.3 (C_1), 55.3 (C_{10}).

Polymerisation of Triol-citro and DCI. *Solvent-free method.* A typical melt polycondensation experiment (#6, Table 1) was performed as follows. Under N_2 atmosphere, Triol-citro (250 mg, 0.912 mmol), DCI (359 mg, 1.368 mmol) and 2 mol% of metal-catalyst (cesium carbonate) based on Triol-citro were added into a 10 mL round-bottom flask connected to a vacuum line, equipped with a condensate trap. The reaction mixture was heated from room temperature to 100 °C at a heating rate of about 32 °C/5 min and stirred continuously for 18 h. Then the temperature was gradually increased to 160°C. After 3h of stirring the temperature was further increased to 220 °C and a high vacuum (10^{-3} bar) was then applied for 2 h. The obtained polymer was dissolved in DMSO at room temperature and left to stir during few minutes. This step was followed by dropwise addition of the solution in methanol (~100 mL) under vigorous stirring at ambient temperature. The precipitate was separated from the solution by filtration and dried at ambient temperature for 48 h.

Solution method. A typical solution polycondensation experiment (#14, Table 3) was performed as follows. Triol-citro (250 mg, 0.912 mmol), DCI (359 mg, 1.368 mmol), Cyrene™ (2 M) based on the summation of number of moles of both Triol-citro and DCI, and 2 mol% of metal-catalyst (cesium carbonate) based on Triol-citro were added into a 10 mL round-bottom flask connected to a vacuum line, equipped with a condensate trap. The reaction mixture was heated from room temperature to 100 °C and low vacuum (0.5 bar) was then applied for 18 h. The temperature and vacuum were gradually increased to 180 °C and 0.2 bar respectively, then the polymerisation reaction was left to stir for 2 h. The temperature was then raised to 200 °C accompanied by an increase in vacuum to 6 mbar for 4 h. The obtained polymer was dissolved in DMSO at room temperature and left to stir during few minutes. This step was followed by dropwise addition of the solution in methanol (~100 mL) under vigorous stirring at ambient temperature. The precipitate was separated from the solution by filtration and dried at ambient temperature for 48 h.

The ^{1}H and ^{13}C NMR (DMSO-d_6) spectra of the polycarbonate obtained are provided in Figures S7 and S8 in the Supporting Information.

UV crosslinking experiment

PC-6 (#6, Table 1) was crosslinked using a 400 W source of UV irradiation (300 nm) in a Rayonet Photochemical Reactor. A 200 mg sample was UV irradiated for 1, 2, 3, 4, 5, and 6 h. Few mgs were taken for each time point to analyze the crosslinked polymers by ^{1}H NMR. The crosslinked material was then analysed by SEC, DSC and TGA.

Conflicts of interest

There are no conflicts to declare.

Acknowledgements

The authors are grateful to the Circa group for its generous gift of LGO, and to Grand Reims, Département de la Marne and Grand Est region for financial support. Fabio Aricò would like to acknowledge the Organization for the Prohibition of Chemical Weapons (OPCW) for partially sponsoring this work; Project Number L/ICA/ICB/218789/19.

Notes and references

1 M. A. Dubé and S. Salehpour, *Macromolecular Reaction Engineering*, 2014, **8**, 7–28.
2 K. N. Onwukamike, S. Grelier, E. Grau, H. Cramail and M. A. R. Meier, *ACS Sustainable Chem. Eng.*, 2019, **7**, 1826–1840.
3 S. Fadlallah, P. Sinha Roy, G. Garnier, K. Saito and F. Allais, *Green Chem.*, 2021, **23**, 1495–1535.
4 P. Anastas and N. Eghbali, *Chem. Soc. Rev.*, 2009, **39**, 301–312.
5 F. H. Isikgor and C. R. Becer, *Polym. Chem.*, 2015, **6**, 4497–4559.
6 N. Tripathi, C. D. Hills, R. S. Singh and C. J. Atkinson, *npj Clim Atmos Sci*, 2019, **2**, 1–10.
7 R. Mülhaupt, *Macromolecular Chemistry and Physics*, 2013, **214**, 159–174.
8 D. Kyriacos, in *Brydson's Plastics Materials (Eighth Edition)*, ed. M. Gilbert, Butterworth-Heinemann, 2017, pp. 457–485.
9 S. Kumar, B. Lively, L. L. Sun, B. Li and W. H. Zhong, *Carbon*, 2010, **48**, 3846–3857.
10 J. L. DeRudder, in *Handbook of Polycarbonate Science and Technology*, CRC Press, 2000.
11 M. W. Hellums, W. J. Koros, G. R. Husk and D. R. Paul, *Journal of Membrane Science*, 1989, **46**, 93–112.
12 S. V. Levchik and E. D. Weil, *Polymer International*, 2005, **54**, 981–998.
13 J. Feng, R.-X. Zhuo and X.-Z. Zhang, *Progress in Polymer Science*, 2012, **37**, 211–236.
14 Polycarbonates global and European production 2016, https://www.statista.com/statistics/650318/polycarbonates-production-worldwide-and-in-europe/, (accessed August 10, 2021).
15 S. Fukuoka, I. Fukawa, T. Adachi, H. Fujita, N. Sugiyama and T. Sawa, *Org. Process Res. Dev.*, 2019, **23**, 145–169.
16 E. J. Hoekstra and C. Simoneau, *Critical Reviews in Food Science and Nutrition*, 2013, **53**, 386–402.
17 S. Cui, J. Borgemenke, Y. Qin, Z. Liu and Y. Li, in *Advances in Bioenergy*, eds. Y. Li and X. Ge, Elsevier, 2019, vol. 4, pp. 183–208.
18 G. W. Coates and D. R. Moore, *Angewandte Chemie International Edition*, 2004, **43**, 6618–6639.
19 W. Zhu, X. Huang, C. Li, Y. Xiao, D. Zhang and G. Guan, *Polymer International*, 2011, **60**, 1060–1067.
20 R. M. de Almeida, J. Li, C. Nederlof, P. O'Connor, M. Makkee and J. A. Moulijn, *ChemSusChem*, 2010, **3**, 325–328.
21 M. J. Climent, A. Corma and S. Iborra, *Green Chem.*, 2011, **13**, 520–540.
22 F. Aricò and P. Tundo, *Beilstein J. Org. Chem.*, 2016, **12**, 2256–2266.
23 F. Aricò, *Current Opinion in Green and Sustainable Chemistry*, 2020, **21**, 82–88.
24 Z. Zhang, W. Lai, L. Su and G. Wu, *Ind. Eng. Chem. Res.*, 2018, **57**, 4824–4831.
25 Z. Zhang, F. Xu, H. He, W. Ding, W. Fang, W. Sun, Z. Li and S. Zhang, *Green Chem.*, 2019, **21**, 3891–3901.
26 C. Vilela, A. F. Sousa, A. C. Fonseca, A. C. Serra, J. F. J. Coelho, C. S. R. Freire and A. J. D. Silvestre, *Polym. Chem.*, 2014, **5**, 3119–3141.
27 M. D. Zenner, Y. Xia, J. S. Chen and M. R. Kessler, *ChemSusChem*, 2013, **6**, 1182–1185.
28 M. Rose and R. Palkovits, *ChemSusChem*, 2012, **5**, 167–176.
29 Q. Li, W. Zhu, C. Li, G. Guan, D. Zhang, Y. Xiao and L. Zheng, *Journal of Polymer Science Part A: Polymer Chemistry*, 2013, **51**, 1387–1397.
30 J. R. Ochoa-Gómez, S. Gil-Río, B. Maestro-Madurga, O. Gómez-Jiménez-Aberasturi and F. Río-Pérez, *Arabian Journal of Chemistry*, 2019, **12**, 4764–4774.
31 W. Fang, Z. Zhang, Z. Yang, Y. Zhang, F. Xu, C. Li, H. An, T. Song, Y. Luo and S. Zhang, *Green Chem.*, 2020, **22**, 4550–4560.
32 Z. Yang, X. Li, F. Xu, W. Wang, Y. Shi, Z. Zhang, W. Fang, L. Liu and S. Zhang, *Green Chemistry*, 2021, **23**, 447–456.
33 W. Qian, X. Ma, L. Liu, L. Deng, Q. Su, R. Bai, Z. Zhang, H. Gou, L. Dong, W. Cheng and F. Xu, *Green Chem.*, 2020, **22**, 5357–5368.
34 Z. Yang, L. Liu, H. An, C. Li, Z. Zhang, W. Fang, F. Xu and S. Zhang, *ACS Sustainable Chem. Eng.*, 2020, **8**, 9968–9979.
35 M. Annatelli, D. D. Torre, M. Musolino and F. Aricò, *Catal. Sci. Technol.*, 2021, **11**, 3411–3421.
36 J.-C. Corpart and R. Saint-Loup, World Intellectual Property Organization, WO2019077250A1, 2019.
37 J.-C. Corpart and R. Saint-Loup, World Intellectual Property Organization, WO2019077252A1, 2019.
38 J.-C. Corpart and R. Saint-Loup, World Intellectual Property Organization, WO2019077228A1, 2019.
39 M. Ibert, E. Josien and H. Wyart, World Intellectual Property Organization, WO2012136942A1, 2012.
40 M. A. Gauthier, M. I. Gibson and H.-A. Klok, *Angewandte Chemie International Edition*, 2009, **48**, 48–58.
41 C. Liu, Z. Jiang, J. Decatur, W. Xie and R. A. Gross, *Macromolecules*, 2011, **44**, 1471–1479.
42 A. Kayishaer, S. Fadlallah, L. M. M. Mouterde, A. A. M. Peru, Y. Werghi, F. Brunois, Q. Carboué, M. Lopez and F. Allais, *Molecules*, 2021, **26**, 7672.
43 M. S. Ariel, M. Z. Maria and A. S. Rolando, *Current Organic Synthesis*, 2012, **9**, 439–459.
44 O. Oyola-Rivera, J. He, G. W. Huber, J. A. Dumesic and N. Cardona-Martínez, *Green Chem.*, 2019, **21**, 4988–4999.
45 T. Debsharma, Y. Yagci and H. Schlaad, *Angewandte Chemie International Edition*, 2019, **58**, 18492–18495.
46 F. Diot-Néant, E. Rastoder, S. A. Miller and F. Allais, *ACS Sustainable Chem. Eng.*, 2018, **6**, 17284–17293.
47 S. Fadlallah, A. A. M. Peru, L. Longé and F. Allais, *Polym. Chem.*, 2020, **11**, 7471–7475.
48 S. Fadlallah, A. A. M. Peru, A. L. Flourat and F. Allais, *European Polymer Journal*, 2020, **138**, 109980.
49 F. Diot-Néant, L. Mouterde, S. Fadlallah, S. A. Miller and F. Allais, *ChemSusChem*, 2020, **13**, 2613–2620.
50 S. Fadlallah, L. M. M. Mouterde, G. Garnier, K. Saito and F. Allais, in *Sustainability & Green Polymer Chemistry Volume 2: Biocatalysis and Biobased Polymers*, American Chemical Society, 2020, vol. 1373, pp. 77–97.
51 J. L. Nichol, N. L. Morozowich, T. E. Decker and H. R. Allcock, *Journal of Polymer Science Part A: Polymer Chemistry*, 2014, **52**, 2258–2265.
52 J. L. Nichol and H. R. Allcock, *European Polymer Journal*, 2015, **62**, 214–221.
53 S. K. Hahn, S. Jelacic, R. V. Maier, P. S. Stayton and A. S. Hoffman, *Journal of Biomaterials Science, Polymer Edition*, 2004, **15**, 1111–1119.
54 S. Fadlallah, A. L. Flourat, L. M. M. Mouterde, M. Annatelli, A. A. M. Peru, A. Gallos, F. Aricò and F. Allais, *Macromol. Rapid Commun.*, 2021, 2100284.
55 Y. S. Eo, H.-W. Rhee and S. Shin, *Journal of Industrial and Engineering Chemistry*, 2016, **37**, 42–46.
56 J. E. Camp, *ChemSusChem*, 2018, **11**, 3048–3055.
57 P. Ray, T. Hughes, C. Smith, M. Hibbert, K. Saito and G. P. Simon, *Polym. Chem.*, 2019, **10**, 3334–3341.
58 M. Vastano, A. Pellis, C. B. Machado, R. Simister, S. J. McQueen-Mason, T. J. Farmer and L. D. Gomez, *Macromolecular Rapid Communications*, 2019, **40**, 1900361.
59 A. Marathianos, E. Liarou, E. Hancox, J. L. Grace, D. W. Lester and D. M. Haddleton, *Green Chem.*, 2020, **22**, 5833–5837.
60 R. A. Milescu, A. Zhenova, M. Vastano, R. Gammons, S. Lin, C. H. Lau, J. H. Clark, C. R. McElroy and A. Pellis, *ChemSusChem*, 2021, **14**, 3367–3381.